


Communication

Isospecific Polymerization of Halide- and Amino-Substituted Styrenes Using a Bis(phenolate) Titanium Catalyst

Qiyuan Wang ^{1,2}, Zhen Zhang ^{1,3}, Yang Jiang ^{1,2}, Yanfeng Zhang ⁴ , Shihui Li ^{1,2,*}  and Dongmei Cui ^{1,2,*} 

¹ State Key Laboratory of Polymer Physics and Chemistry, Changchun Institute of Applied Chemistry, Chinese Academy of Sciences, Changchun 130022, China; wangqy99@ciac.ac.cn (Q.W.); zzzzhang@ciac.ac.cn (Z.Z.); yjiang@ciac.ac.cn (Y.J.)

² School of Applied Chemistry and Engineering, University of Science and Technology of China, Hefei 230026, China

³ Department of Materials Science and Engineering, Jilin University, Changchun 130022, China

⁴ School of Chemistry, Xi'an Jiaotong University, Xi'an 710049, China; yanfengzhang@mail.xjtu.edu.cn

* Correspondence: shihui-li@ciac.ac.cn (S.L.); dmcui@ciac.ac.cn (D.C.)

Abstract: Isospecific polymerization of polar styrenes is a challenge of polymer science. Particularly challenging are monomers bearing electron-withdrawing substituents or bulky substituents. Here, we report the coordination polymerization of halide- and amino-functionalized styrenes including *para*-fluorostyrene (*p*FS), *para*-chlorostyrene (*p*ClS), *para*-bromostyrene (*p*BrS), and *para*-(*N,N*-diethylamino)styrene (DMAS) using 2,2'-sulfur-bridged bis(phenolate) titanium precursor (**1**). The combination of **1** and [Ph₃C][B(C₆F₅)₄] and Al^{*i*}Bu₃ provides crystalline poly(*p*FS)s with perfect isotacticity (*mmmm* > 95%) and high molecular weights ($\leq 16.0 \times 10^4$ g mol⁻¹). Upon activation with a large excess of DMAO, **1** reaches polymerization activity of 5.58×10^5 g mol⁻¹ h⁻¹ producing isotactic poly(*p*FS)s featuring higher molecular weights ($\leq 39.6 \times 10^4$ g mol⁻¹). The distinguished performance of the **1**/DMAO system has been extended to the polymerization of *p*ClS and *p*BrS, both usually involve halogen abstraction during the polymerization, to produce isotactic and high molecular weight ($M_n = 32.2 \times 10^4$ vs. 13.7×10^4 g mol⁻¹) polymers in good activities (2.18×10^5 vs. 1.31×10^5 g mol⁻¹ h⁻¹). Surprisingly, **1**/DMAO is nearly inactive for DMAS polymerization, on contrary, the system **1**/[Ph₃C][B(C₆F₅)₄]/Al^{*i*}Bu₃ displays isoselectivity (*mmmm* > 95%) albeit in a moderate activity.

Keywords: isospecific polymerization; halostyrene; amino-substituted styrene; titanium complex



Citation: Wang, Q.; Zhang, Z.; Jiang, Y.; Zhang, Y.; Li, S.; Cui, D. Isospecific Polymerization of Halide- and Amino-Substituted Styrenes Using a Bis(phenolate) Titanium Catalyst. *Catalysts* **2022**, *12*, 439. <https://doi.org/10.3390/catal12040439>

Academic Editor: Bun Yeoul Lee

Received: 15 March 2022

Accepted: 12 April 2022

Published: 13 April 2022

Publisher's Note: MDPI stays neutral with regard to jurisdictional claims in published maps and institutional affiliations.



Copyright: © 2022 by the authors. Licensee MDPI, Basel, Switzerland. This article is an open access article distributed under the terms and conditions of the Creative Commons Attribution (CC BY) license (<https://creativecommons.org/licenses/by/4.0/>).

1. Introduction

The stereoselective polymerization of styrenes has made significant progress in recent years due to the development of novel transition metal catalysts [1–5] since Ishihara et al. first discovered that half-sandwich titanium complexes could catalyse the syndiospecific polymerization of styrene in 1985 [6,7]. Much effort has been expended pursuing the synthesis of stereospecific catalysts for the (co)polymerization of styrene derivatives bearing polar groups [8–12], such as halogen [13–17], alkoxy [18–23], aminoalkyl [24–26], etc., which will endow the resultant polymers with distinguished functionalities such as improved surface properties, self-healing, and shape-memory abilities [27–31]. Group 4 metal-based catalysts have achieved some limited success in the polymerization of polar styrenes because they are easily poisoned by the polar groups [32–34]. The half-titanocene Cp*Ti(TEA)/MMAO is reported to show high catalytic activity and perfect syndiospecificity for the polymerization of amino-functionalized styrenes [35]. Ti(CH₂Ph)₄/MAO catalyses *para*-methoxystyrene polymerization with low activity, to give an atactic polymer [36]. With respect to the polymerization of halostyrene, titanium catalysts usually produce atactic polymers or a mixture of atactic and syndiotactic polymers, albeit with low catalytic activity [37–40]. Recently, the group-3 half-sandwich scandium complexes, especially those rare-earth metal-based

complexes attached to the constrained geometry pyridyl-methylene-fluorenyl ligands, have shown excellent catalytic activity towards a broad range of polar styrenes to give syndiotactic polymers [5,8].

In contrast, the isotactic polymerization of polar styrene monomers develops relatively slowly [17,41], mainly due to the lack of highly efficient catalysts, which struggle to provide high activity while maintaining the sterically crowded coordination sphere required by the isotactic selectivity, although isotactic-enriched polystyrene has been synthesized long before with Ziegler–Natta catalysts or anionic catalysts [42,43]. However, the potential applications of functionalized isotactic polystyrenes as optically active, helical, etc., functional materials have led researchers to expend a lot of effort in this research field. In 2015, the first homogeneous single-site β -diketiminato rare-earth metal catalysts were developed by our group, showing high isoselectivity for *ortho*-methoxystyrene without masking reagents via the unique “self-assisted” mechanism; however, they are nearly inactive towards other polar styrene derivatives [44,45]. Recently, we developed a series of *racemic* isopropylidene-bridged bis(benz[e]indenyl) rare-earth metal alkyl complexes, which served as effective catalysts for the isoselective polymerizations of styrene, *para/meta*-methoxystyrenes, *para*-methylthiostyrene, and *para*-vinylphenyldimethylsilanol, etc. [46]. Unfortunately, they were virtually inert to the halide- and amino-functionalized styrenes. Probably because the coordination sphere of these catalysts is more open to allow more monomer coordination, in particular in the inert $M-\sigma-X$ (X = functional group) mode. The bulkier *ansa*-bridged bis(indenyl) allyl yttrium and neodymium complexes developed by Carpentier’s group are also inactive [47,48], where the vacant coordination site is too crowded to facilitate the coordination of bulky amino-functionalized styrenes. In addition, the low Lewis acidity of neutral catalysts inhibits the coordination of the electron-deficient double bond of halostyrene to the metal ion. Thus, we turned to the 2,2′-sulfur-bridged bis(phenolato) titanium dichloro complex with a higher Lewis acidity (**1**) (Figure 1) [49–52], an isospecific catalyst for styrene polymerization reported by Okuda and co-workers, and examined its catalytic performance for the polymerization of polar styrenes, and in particular, of halostyrenes, since the resultant halogen styrene polymers feature improved corrosion resistance, heat resistance, flame retardancy, etc. [53–57]. Moreover, the halogen groups can be easily converted into other functionalities to impart different properties to the polymers [58]. In addition, this catalyst performs well in catalysing the (co)polymerization of conjugated dienes [59,60], which provides a possible route for the direct synthesis of halide-functionalized butyl rubber with faster vulcanization, high energy absorption, and low elastic modulus [61,62], and halide-functionalized butadiene-styrene rubber possessing better compatibility with polar fillers which could be used to fabricate tires with low-rolling resistance and good wet-skid resistance [63–66]. Herein, we report the polymerization behaviour of *para*-fluorostyrene (*p*FS), *para*-chlorostyrene (*p*ClS), *para*-bromostyrene (*p*BrS), and *para*-(*N,N*-diethylamino)styrene (DMAS) by using complex **1** activated by organoborate, alkyl aluminium, MAO and dried MAO (DMAO).

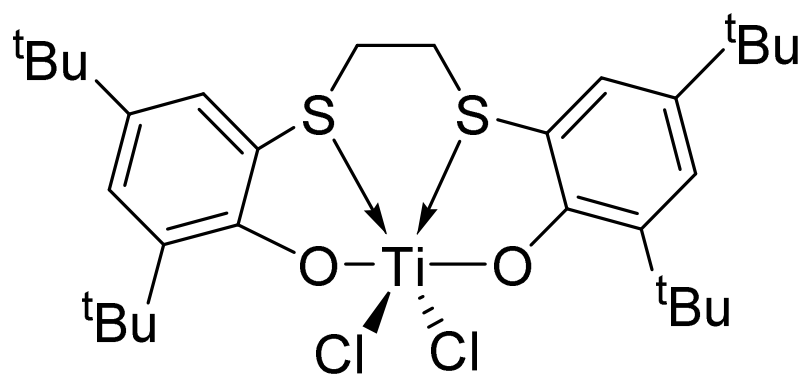


Figure 1. Structure of [OSSO]-type titanium complex **1**.

2. Results and Discussion

At first, a combination of **1** with $[\text{Ph}_3\text{C}][\text{B}(\text{C}_6\text{F}_5)_4]$ and Al^iBu_3 was chosen as the catalyst for polymerization of *para*-fluorostyrene (*p*FS) because organoborate-based activators are reported to be more efficient reagents than MAO. The polymerization was performed at 25 °C in a toluene solution to reach 54% conversion in 30 min. On increasing the reaction temperature from 25 to 80 °C, the highest catalytic activity of $1.12 \times 10^5 \text{ g mol}^{-1} \text{ h}^{-1}$ was observed at 40 °C (Table 1, entries 1–4), probably because the Ti(IV) active species is readily reduced to the inert Ti(III) by aluminium alkyls at high reaction temperatures. Subsequently, a kinetics investigation was carried out at 40 °C under a *p*FS-to-**1** ratio of 1000:1. Increasing the reaction time from 15 to 120 min resulted in an obvious increase in monomer conversion from 30% to 79% (Table 1, entries 5–7). The molecular weight distributions of the resultant polymers consequently broadened from 1.53 to 1.89, but the molecular weights ($M_n = 15.1\text{--}16.0 \times 10^4 \text{ g mol}^{-1}$) remained nearly constant (Figure 2), indicating the chain transfer reaction accompanying the polymerization process.

Table 1. Isoselective polymerization of *p*FS with complex **1**, Al^iBu_3 and $[\text{Ph}_3\text{C}][\text{B}(\text{C}_6\text{F}_5)_4]$.

Entry ¹	[<i>p</i> FS]/[Ti] [mol/mol]	Time [min]	Temp. [°C]	Conv. [%]	Act. ²	M_n ³ [$\times 10^4$]	M_w/M_n ³	<i>mmmm</i> ⁴ [%]	T_g/T_m ⁵ [°C]
1	500/1	30	25	54	0.66	15.5	1.60	>95	103.5/253.7
2	500/1	30	40	91	1.12	9.9	1.58	>95	103.4/240.7
3	500/1	30	60	42	0.51	5.7	1.76	>95	102.1/236.1
4	500/1	30	80	28	0.34	4.0	1.83	>95	97.8/233.9
5	1000/1	15	40	30	1.47	15.1	1.53	>95	102.7/246.6
6	1000/1	35	40	59	1.24	16.0	1.81	>95	104.4/243.1
7	1000/1	120	40	79	0.48	15.8	1.89	>95	99.7/237.4

¹ General conditions: complex **1**, 10 μmol ; $[\text{Ti}]/[\text{Ph}_3\text{C}][\text{B}(\text{C}_6\text{F}_5)_4]/[\text{Al}^i\text{Bu}_3] = 1/1/30 \text{ (mol/mol/mol)}$; [*p*FS] = 3.125 mol/L in toluene solution; ² Given in $10^5 \text{ g mol}^{-1} \text{ h}^{-1}$; ³ Determined by GPC in 1,2,4-trichlorobenzene at 150 °C against polystyrene standard; ⁴ Determined by ^1H and ^{13}C NMR; ⁵ Determined by DSC.

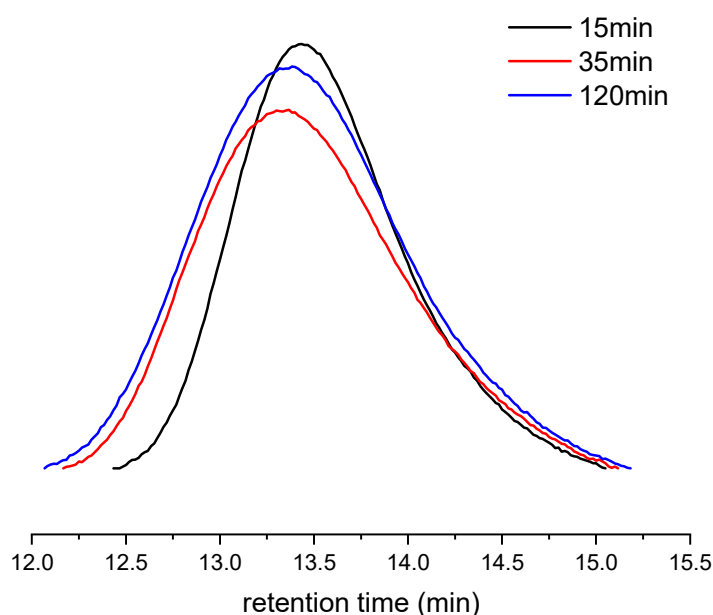
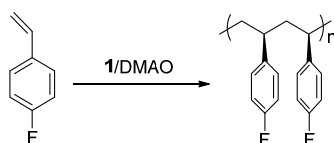


Figure 2. GPC curves of poly(*p*FS)s obtained at different polymerization time (Table 1, entries 5–7).

The catalytic system **1**/MAO has been reported to exhibit high catalytic activity for isospecific styrene polymerization [49]. Therefore, complex **1** activated by 2000 equivalents of MAO was utilized to catalyse *p*FS polymerization at 40 °C; however, only 25% of the monomer was consumed in 2 h (Table 2, entry 1). In contrast, the combination of **1** and 2000 equivalents of DMAO showed a much higher catalytic activity ($5.51 \times 10^5 \text{ g mol}_{\text{Ti}}^{-1} \text{ h}^{-1}$ vs. $1.51 \times 10^5 \text{ g mol}_{\text{Ti}}^{-1} \text{ h}^{-1}$) with 90% monomer conversion under identical conditions (Table 2, entry 2). This was attributed mainly to the absence of free AlMe_3 , which is able to interact with the active species leading to an inactive dimethyl-bridged species [67–69]. Notably, a large excess of DMAO against complex **1** is necessary in order to obtain a highly active species for *p*FS polymerization. Whenever all complex **1** molecules were converted into the cationic active species, further increasing DMAO loading amount did not improve the catalytic activity (Table 2, entries 2, 6, and 7). Increasing reaction temperature accelerated the polymerization process to a certain degree, but too-high a temperature led to declined polymerization activity from $5.51 \times 10^5 \text{ g mol}_{\text{Ti}}^{-1} \text{ h}^{-1}$ at 40 °C to $4.54 \times 10^5 \text{ g mol}_{\text{Ti}}^{-1} \text{ h}^{-1}$ at 60 °C, along with a dramatic decrease in molecular weight from $37.4 \times 10^5 \text{ g mol}_{\text{Ti}}^{-1}$ to $13.4 \times 10^5 \text{ g mol}_{\text{Ti}}^{-1} \text{ h}^{-1}$ (Table 2, entries 2, 8 and 9).

Table 2. Isospecific polymerization of *p*FS with complex **1** and DMAO.



Entry ¹	[<i>p</i> FS]/[Ti]/[Al] [mol/mol/mol]	Temp. [°C]	Conv. [%]	Act. ²	<i>M_n</i> ³ [$\times 10^4$]	<i>M_w</i> / <i>M_n</i> ³	<i>mmmm</i> ⁴ [%]	<i>T_g</i> / <i>T_m</i> ⁵ [°C]
1 ⁶	10,000/1/2000	40	25	1.51	8.4	1.71	>95	101.2/244.4
2	10,000/1/2000	40	90	5.51	37.4	1.81	>95	105.2/245.6
3	10,000/1/500	40	61	3.70	37.3	1.96	>95	103.9/247.8
4	10,000/1/1000	40	73	4.48	35.1	1.97	>95	104.1/244.1
5	10,000/1/1500	40	80	4.90	35.3	1.99	>95	104.2/245.1
6	10,000/1/2500	40	91	5.58	39.6	1.72	>95	104.5/242.9
7	10,000/1/3000	40	91	5.58	34.7	1.77	>95	104.8/243.2
8	10,000/1/2000	25	81	4.95	38.4	1.66	>95	104.1/250.2
9	10,000/1/2000	60	74	4.54	13.4	1.81	>95	103.4/-

¹ General conditions: complex **1**, 1 μmol ; polymerization time, 120 min; [*p*FS] = 3.125 mol/L in toluene solution; dried MAO is used as cocatalyst; ² Given in $10^5 \text{ g mol}_{\text{Ti}}^{-1} \text{ h}^{-1}$; ³ Determined by GPC in 1,2,4-trichlorobenzene at 150 °C against polystyrene standard; ⁴ Determined by ^1H and ^{13}C NMR; ⁵ Determined by DSC; ⁶ MAO is used as cocatalyst.

All of the resulting poly(*p*FS)s are nearly insoluble in toluene, tetrahydrofuran (THF), chloroform, etc., at room temperature, but readily soluble in chlorobenzene, acetylene tetrachloride, etc., at high temperature. NMR spectroscopy analysis unambiguously indicated that the poly(*p*FS)s produced by both the catalytic systems **1**/ Al^iBu_3 / $[\text{Ph}_3\text{C}][\text{B}(\text{C}_6\text{F}_5)_4]$ and **1**/DMAO have an isotactic microstructure, evidenced by the quintet centred at δ 2.14 ppm and the multiplet centred at δ 1.52 ppm assigned to the methine and asymmetric methylene protons, respectively (Figure 3a). The perfect isotacticity is further confirmed by the sharp singlets at δ 43.78 ppm for methylene carbon and δ 41.03 ppm for methine carbon. All the peaks of the fluorine-substituted phenyl carbons split into doublets as a result of coupling with ^{19}F nuclei (Figure 3b). The *ipso*-carbon C3 shows a doublet at δ 141.62 ppm with a coupling constant of $^4J_{\text{C-F}} = 3 \text{ Hz}$. The coupling constants of *ortho*-carbon C4 (δ 128.94 ppm, $^3J_{\text{C-F}} = 8 \text{ Hz}$), *meta*-carbon C5 (δ 115.12 ppm, $^2J_{\text{C-F}} = 21 \text{ Hz}$) and *para*-carbon C6 (δ 161.55 ppm, $^1J_{\text{C-F}} = 244 \text{ Hz}$) are significantly enlarged due to gradually closing to the fluorine atom. The obtained isotactic polymer shows a high glass-transition temperature of around 104 °C and a melting temperature in the range of 242.9–247.8 °C (Figure S20–S28), which are much lower than those observed in syndiotactic poly(*p*FS) [14].

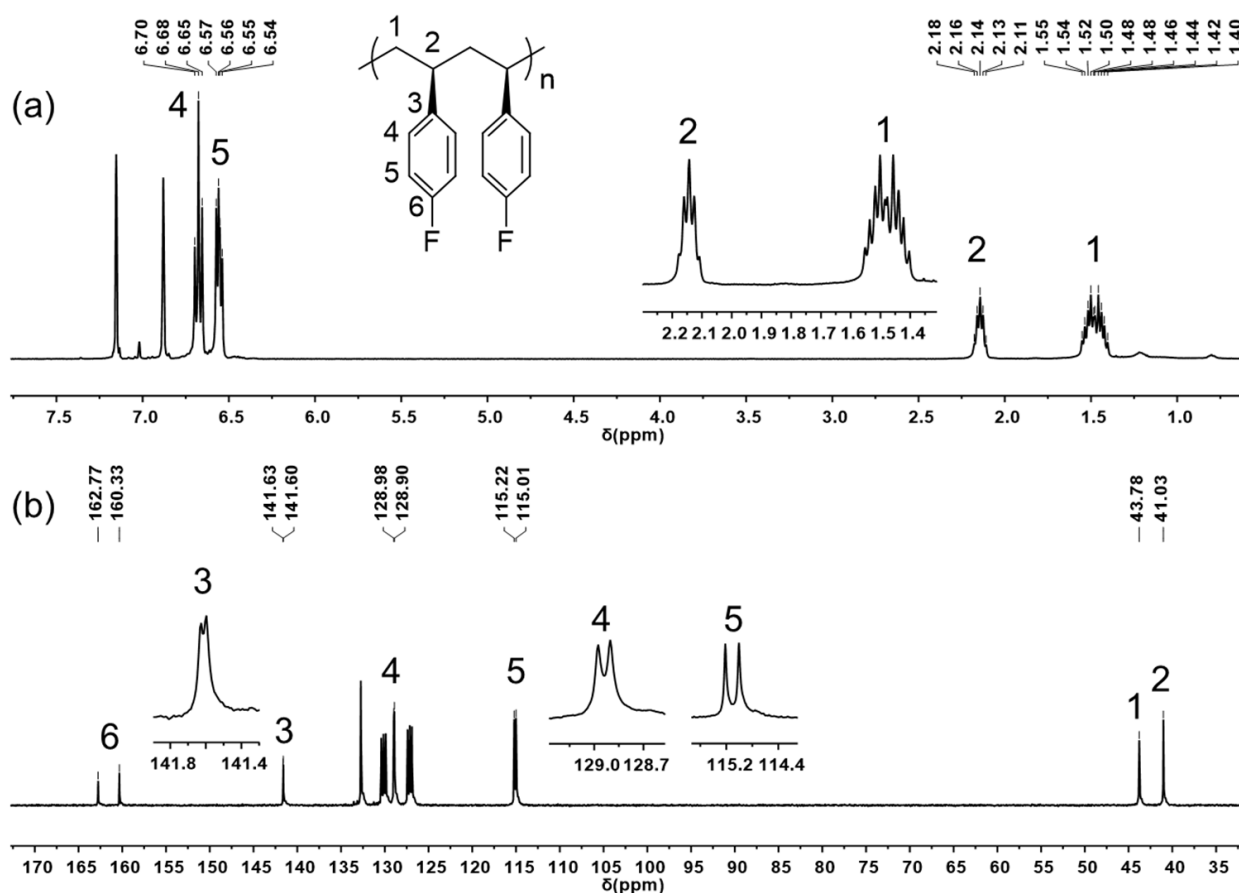


Figure 3. ^1H NMR spectrum (a) and ^{13}C NMR spectrum (b) of isotactic poly(*p*FS) ($\text{C}_6\text{Cl}_2\text{D}_4$, 110°C) (Table 1, entry 2).

Stimulated by the above results, the polymerizations of other chloro-styrene derivatives were studied using the system **1**/DMAO. In a previous report, chloro- and bromo-substituted styrenes needed to be polymerized at low temperatures ($\leq 0^\circ\text{C}$) because the scandium cationic active species readily cleaved the C-X ($\text{X} = \text{Cl}$ or Br) bond of halostyrene to generate the inert metal-halide species at high temperatures [15]. Surprisingly to us, *para*-chlorostyrene (*p*ClS) was also converted into a perfect isotactic polymer at 40°C with 63% conversion in 2 h (Table 3, entry 1). This may be due to the Lewis acidity of titanium cationic active species being lower than that of scandium, which would not cause C-X bond cleavage at higher temperatures. Even *para*-bromostyrene (*p*BrS) polymerization under similar conditions reached 57% monomer conversion in a prolonged reaction time (4 h) (Table 3, entry 2). Their polymerization activities relate mainly to the electronics of the monomers following the trend $p\text{FS} > p\text{ClS} > p\text{BrS}$, which is consistent with the natural bond orbital (NBO) charge of $\beta\text{-CH}_2$ of these monomers; *p*BrS has the lowest electron density (-0.339) as compared to *p*ClS (-0.346) and *p*FS (-0.353) (Figure S38). On the other hand, Cl and Br atoms with larger atomic radii may also adversely affect the polymerization. Unexpectedly, **1**/DMAO was virtually inactive for the polymerization of *para*-(*N,N*-diethylamino)styrene (DMAS). Switching to the catalytic system of **1**/ Al^iBu_3 /[Ph_3C][$\text{B}(\text{C}_6\text{F}_5)_4$], surprisingly, effective polymerization was achieved by converting 82% DMAS in 30 min in an isospecific manner, although the bulky dimethylamino group significantly decreased the activity (Table 3, entry 4). Thermal analyses revealed all the resultant isotactic poly(*p*ClS), poly(*p*BrS), and poly(DMAS) possess higher glass transition temperatures of 124.7 , 135.1 , and 130.7°C , respectively, but the melting points were not observed in the DSC curves despite their perfect isotacticity ($mmmm > 95\%$) (Figure S39–S43).

Table 3. Isoselective polymerization of styrene derivatives with complex 1.

Entry ¹	[M]	[pFS]/[Ti] [mol/mol]	Time [min]	Temp. [°C]	Conv. [%]	Act. ²	M_n ³ [$\times 10^4$]	M_w/M_n ³	mmmm ⁴ [%]	T_g/T_m ⁵ [°C]
1	pClS	5000/1	120	40	63	2.18	32.2	2.06	>95	124.7/-
2	pBrS	5000/1	240	40	57	1.31	13.7	2.08	>95	135.1/-
3	DMA	5000/1	90	40	trace	-	-	-	-	-
4 ⁶	DMA	200/1	30	40	82	0.32	7.5	1.37	>95	130.7/-

¹ General conditions: complex 1, 1 μ mol; [Ti]/[DMAO] = 1/2000 (mol/mol); toluene, 1.6 mL; ² Given in 10^5 g mol⁻¹ h⁻¹; ³ Determined by GPC in 1,2,4-trichlorobenzene at 150 °C against polystyrene standard; ⁴ Determined by ¹H and ¹³C NMR; ⁵ Determined by DSC; ⁶ complex 1, 10 μ mol; [Ti]/[Ph₃C][B(C₆F₅)₄]/[AlⁱBu₃] = 1/1/30 (mol/mol/mol).

3. Conclusions

We have demonstrated that the isospecific polymerizations of halostyrene and amino-functionalized styrenes with high activity have been achieved using titanium bisphenolate catalyst 1. Compared with scandium, yttrium, and lutetium rare-earth metal-based catalysts, titanium catalysts have suitable Lewis acidity, which not only compensates for the low coordination ability of the double bond on halostyrenes, but also does not cause C-X bond cleavage at high temperatures. The polymerization activity is strongly influenced by the co-catalysts and the reaction temperature. Upon activation with AlⁱBu₃ and [Ph₃C][B(C₆F₅)₄], complex 1 furnishes perfect isospecific poly(pFS) with high molecular weight and narrow molecular weight distribution for the first time; however, the polymerization activity is relatively low. When DMAO is used as the cocatalyst, the pFS polymerization process is greatly accelerated under a suitable reaction temperature, resulting in an isotactic product with a higher molecular weight and a narrow molecular weight distribution. A reaction temperature over 40 °C is not detrimental to isoselectivity but decreases the polymerization activity and the molecular weight, probably due to the reduction of Ti (IV) to Ti (III) by alkyl aluminium and the chain transfer reaction. In addition, the combination of 1/DMAO also shows high catalytic activity and perfect isoselectivity for the polymerization of pClS and pBrS, but the isospecific polymerization of DMA is only accomplished by the system 1/[Ph₃C][B(C₆F₅)₄]/AlⁱBu₃. This work paves a new avenue to access isotactic polyhalostyrenes, which can be easily transferred to other functionalized isotactic polystyrenes.

Supplementary Materials: The following supporting information can be downloaded at: <https://www.mdpi.com/article/10.3390/catal12040439/s1>, Experimental procedures; Figure S1: ¹H NMR spectrum of poly(pFS) (400MHz, C₆Cl₂D₄, 110 °C) (Table 1, entry 1); Figure S2: ¹³C NMR spectrum of poly(pFS) (100MHz, C₆Cl₂D₄, 110 °C) (Table 1, entry 1); Figure S3: ¹H NMR spectrum of poly(pFS) (400MHz, C₆Cl₂D₄, 110 °C) (Table 1, entry 3); Figure S4: ¹³C NMR spectrum of poly(pFS) (100MHz, C₆Cl₂D₄, 110 °C) (Table 1, entry 3); Figure S5: ¹H NMR spectrum of poly(pFS) (400MHz, C₆Cl₂D₄, 110 °C) (Table 1, entry 4); Figure S6: ¹³C NMR spectrum of poly(pFS) (100MHz, C₆Cl₂D₄, 110 °C) (Table 1, entry 4); Figure S7: The DSC curve of poly(pFS) (Table 1, entry 1); Figure S8: The DSC curve of poly(pFS) (Table 1, entry 2); Figure S9: The DSC curve of poly(pFS) (Table 1, entry 3); Figure S10: The DSC curve of poly(pFS) (Table 1, entry 4); Figure S11: The DSC curve of poly(pFS) (Table 1, entry 5); Figure S12: The DSC curve of poly(pFS) (Table 1, entry 6); Figure S13: The DSC curve of poly(pFS) (Table 1, entry 7); Figure S14: The GPC curve of poly(pFS) (Table 1, entry 1); Figure S15: The GPC curve of poly(pFS) (Table 1, entry 2); Figure S16: The GPC curve of poly(pFS) (Table 1, entry 3); Figure S17: The GPC curve of poly(pFS) (Table 1, entry 4); Figure S18: ¹H NMR spectrum of poly(pFS) (400MHz, C₆Cl₂D₄, 110 °C) (Table 2, entry 2); Figure S19: ¹³C NMR spectrum of poly(pFS) (100MHz, C₆Cl₂D₄, 110 °C) (Table 2, entry 2); Figure S20: The DSC curve of poly(pFS) (Table 2, entry 1); Figure S21: The DSC curve of poly(pFS) (Table 2, entry 2); Figure S22: The DSC curve of poly(pFS) (Table 2, entry 3); Figure S23: The DSC curve of poly(pFS) (Table 2, entry 4); Figure S24: The DSC curve of poly(pFS) (Table 2, entry 5); Figure S25: The DSC curve of poly(pFS) (Table 2, entry 6); Figure S26: The DSC curve of poly(pFS) (Table 2, entry 7); Figure S27: The DSC curve of poly(pFS) (Table 2, entry 8); Figure S28: The DSC curve of poly(pFS) (Table 2, entry 9); Figure S29: The GPC curve of poly(pFS) (Table 2, entry 1); Figure S30: The GPC curve of poly(pFS) (Table 2, entry 2); Figure S31: The GPC curve of poly(pFS) (Table 2, entry 3); Figure S32: The GPC curve of poly(pFS) (Table 2, entry 4); Figure S33:

The GPC curve of poly(*p*FS) (Table 2, entry 5); Figure S34: The GPC curve of poly(*p*FS) (Table 2, entry 6); Figure S35: The GPC curve of poly(*p*FS) (Table 2, entry 7); Figure S36: The GPC curve of poly(*p*FS) (Table 2, entry 8); Figure S37: The GPC curve of poly(*p*FS) (Table 2, entry 9); Figure S38: NBO charge of the monomers. (a) St; (b) *p*FS; (c) *p*ClS; (d) *p*BrS; Figure S39: ¹H NMR spectrum of poly(*p*ClS) (400MHz, C₆Cl₂D₄, 110 °C) (Table 3, entry 1); Figure S40: ¹³C NMR spectrum of poly(*p*ClS) (100MHz, C₆Cl₂D₄, 110 °C) (Table 3, entry 1); Figure S41: ¹H NMR spectrum of poly(*p*BrS) (400MHz, C₆Cl₂D₄, 110 °C) (Table 3, entry 2); Figure S42: ¹³C NMR spectrum of poly(*p*BrS) (100MHz, C₆Cl₂D₄, 110 °C) (Table 3, entry 2); Figure S43: ¹³C NMR spectrum of poly(DMAS) (100MHz, CDCl₃, 25 °C) (Table 3, entry 4); Figure S44: The DSC curve of poly(*p*ClS) (Table 3, entry 1); Figure S45: The DSC curve of poly(*p*BrS) (Table 3, entry 2); Figure S46: The DSC curve of poly(DMAS) (Table 3, entry 4); Figure S47: The GPC curve of poly(*p*ClS) (Table 3, entry 1); Figure S48: The GPC curve of poly(*p*BrS) (Table 3, entry 2); Figure S49: The GPC curve of poly(DMAS) (Table 3, entry 4).

Author Contributions: Conceptualization, Q.W. and S.L.; methodology, Q.W., Z.Z. and Y.J.; formal analysis, Q.W. and S.L.; investigation, Q.W. and Z.Z.; resources, D.C.; data curation, Q.W.; writing—original draft preparation, Q.W. and S.L.; writing—review and editing, S.L. and D.C.; project administration, S.L. and D.C.; funding acquisition, S.L., Y.Z. and D.C. All authors have read and agreed to the published version of the manuscript.

Funding: This research was funded by Department of Science and Technology of Shanxi Province, grant number 2021JLM-40 and the National Natural Science Foundation of China, grant number 52073275.

Data Availability Statement: The data presented in this study are available in Supplementary Materials.

Conflicts of Interest: The authors declare no conflict of interest.

References

- Kirillov, E.; Lehmann, C.W.; Razavi, A.; Carpentier, J.F. Highly Syndiospecific Polymerization of Styrene Catalyzed by Allyl Lanthanide Complexes. *J. Am. Chem. Soc.* **2004**, *126*, 12240–12241. [[CrossRef](#)] [[PubMed](#)]
- Luo, Y.; Baldamus, J.; Hou, Z. Scandium Half-Metallocene-Catalyzed Syndiospecific Styrene Polymerization and Styrene–Ethylene Copolymerization: Unprecedented Incorporation of Syndiotactic Styrene–Styrene Sequences in Styrene–Ethylene Copolymers. *J. Am. Chem. Soc.* **2004**, *126*, 13910–13911. [[CrossRef](#)] [[PubMed](#)]
- Huang, J.; Liu, Z.; Cui, D.; Liu, X. Precisely Controlled Polymerization of Styrene and Conjugated Dienes by Group 3 Single-Site Catalysts. *Chemcatchem* **2018**, *10*, 42–61. [[CrossRef](#)]
- Jaroschik, F.; Shima, T.; Li, X.; Mori, K.; Ricard, L.; Le Goff, X.-F.; Nief, F.; Hou, Z. Synthesis, Characterization, and Reactivity of Mono(phosphoryl)lanthanoid(III) Bis(dimethylaminobenzyl) Complexes. *Organometallics* **2007**, *26*, 5654–5660. [[CrossRef](#)]
- Wu, Z.; Fu, X. Stereospecific Coordination Polymerization of Vinyl Monomers Mediated by Rare earth Metal Complexes. *Sci. Sin. Chim.* **2020**, *50*, 1654–1671. [[CrossRef](#)]
- Ishihara, N.; Seimiya, T.; Kuramoto, M.; Uoi, M. Crystalline Syndiotactic Polystyrene. *Macromolecules* **1986**, *19*, 2464–2465. [[CrossRef](#)]
- Ishihara, N.; Kuramoto, M.; Uoi, M. Stereospecific Polymerization of Styrene Giving the Syndiotactic Polymer. *Macromolecules* **1988**, *21*, 3356–3360. [[CrossRef](#)]
- Cui, D. Studies on Homo- and Co-polymerizations of Polar and Non-polar Monomers Using Rare-earth Metal Catalysts. *Acta. Polym. Sin.* **2020**, *51*, 12–29.
- Liu, D.; Wang, M.; Chai, Y.; Wan, X.; Cui, D. Self-Activated Coordination Polymerization of Alkoxy-styrenes by a Yttrium Precursor: Stereocontrol and Mechanism. *ACS Catal.* **2019**, *9*, 2618–2625. [[CrossRef](#)]
- Li, S.; Liu, D.; Wang, Z.; Cui, D. Development of Group 3 Catalysts for Alternating Copolymerization of Ethylene and Styrene Derivatives. *ACS Catal.* **2018**, *8*, 6086–6093. [[CrossRef](#)]
- Zhang, Z.; Jiang, Y.; Zhang, K.; Cai, Z.; Li, S.; Cui, D. DMAO-activated Rare-earth Metal Catalysts for Styrene and Its Derivative Polymerization. *Chin. J. Polym. Sci.* **2021**, *39*, 1185–1190. [[CrossRef](#)]
- Liu, D.; Wang, R.; Wang, M.; Wu, C.; Wang, Z.; Yao, C.; Liu, B.; Wan, X.; Cui, D. Syndioselective Coordination Polymerization of Unmasked Polar Methoxystyrenes Using a Pyridenylmethylene Fluorenyl Yttrium Precursor. *Chem. Commun.* **2015**, *51*, 4685–4688. [[CrossRef](#)] [[PubMed](#)]
- Guo, F.; Jiao, N.; Jiang, L.; Li, Y.; Hou, Z. Scandium-Catalyzed Syndiospecific Polymerization of Halide-Substituted Styrenes and Their Copolymerization with Styrene. *Macromolecules* **2017**, *50*, 8398–8405. [[CrossRef](#)]
- Wang, Z.; Wang, M.; Liu, J.; Liu, D.; Cui, D. Rapid Syndiospecific (Co)Polymerization of Fluorostyrene with High Monomer Conversion. *Chem. Eur. J.* **2017**, *23*, 18151–18155. [[CrossRef](#)]
- Wu, Y.; Wang, Z.; Liu, D.; Liu, B.; Cui, D. Highly Syndioselective Coordination (Co)Polymerization of *para*-Chlorostyrene. *Macromolecules* **2020**, *53*, 8333–8339. [[CrossRef](#)]

16. Wang, T.; Liu, D.; Cui, D. Highly Syndioselective Coordination (Co)Polymerization of *ortho*-Fluorostyrene. *Macromolecules* **2019**, *52*, 9555–9560. [[CrossRef](#)]
17. Carlo, F.D.; Capacchione, C.; Schiavo, V.; Proto, A. Reactivity of Styrene and Substituted Styrenes in the Presence of A Homogeneous Isospecific Titanium Catalyst. *J. Polym. Sci. Part A Polym. Chem.* **2006**, *44*, 1486–1491. [[CrossRef](#)]
18. Xu, S.; Wang, J.; Zhai, J.; Wang, F.; Pan, L.; Shi, X. Imidazoline-2-imine Functionalized Fluorenyl Rare-Earth Metal Complexes: Synthesis and Their Application in the Polymerization of *ortho*-Methoxystyrene. *Organometallics* **2021**, *40*, 3323–3330. [[CrossRef](#)]
19. Song, C.; Chen, J.; Fu, Z.; Yan, L.; Gao, F.; Cao, Q.; Li, H.; Yan, X.; Chen, S.; Zhang, S.; et al. Syndiospecific Polymerization of *o*-Methoxystyrene and Its Silyloxy or Fluorine-Substituted Derivatives by HNC-Ligated Scandium Catalysts: Synthesis of Ultrahigh-Molecular-Weight Functionalized Polymers. *Macromolecules* **2021**, *54*, 10838–10849. [[CrossRef](#)]
20. Wang, R.; Liu, D.; Li, X.; Zhang, J.; Cui, D.; Wan, X. Synthesis and Stereospecific Polymerization of a Novel Bulky Styrene Derivative. *Macromolecules* **2016**, *49*, 2502–2510. [[CrossRef](#)]
21. Cui, L.; Chen, M.; Chen, C.; Liu, D.; Jian, Z. Systematic Studies on (Co)Polymerization of Polar Styrene Monomers with Palladium Catalysts. *Macromolecules* **2019**, *52*, 7197–7206. [[CrossRef](#)]
22. Li, X.; Wang, R.; Wu, C.; Chen, J.; Zhang, J.; Cui, D.; Wan, X. Effect of the tactic structure on the chiroptical properties of helical vinylbiphenyl polymers. *Polym. Chem.* **2019**, *10*, 3887–3894. [[CrossRef](#)]
23. Shi, X.; Nishiura, M.; Hou, Z. Simultaneous Chain-Growth and Step-Growth Polymerization of Methoxystyrenes by Rare-Earth Catalysts. *Angew. Chem. Int. Ed.* **2016**, *55*, 14812–14817. [[CrossRef](#)] [[PubMed](#)]
24. Mu, X.; Li, Y. Syndiospecific Coordination (Co)polymerization of Carbazole-substituted Styrene Derivatives Using the Scandium Catalyst System. *Polym. Chem.* **2021**, *12*, 6291–6299. [[CrossRef](#)]
25. Jiang, L.; Guo, F.; Shi, Z.; Li, Y.; Hou, Z. Syndiotactic Poly(aminostyrene)-Supported Palladium Catalyst for Ketone Methylation with Methanol. *Chemcatchem* **2017**, *9*, 3827–3832. [[CrossRef](#)]
26. Shi, Z.; Guo, F.; Li, Y.; Hou, Z. Synthesis of Amino-containing Syndiotactic Polystyrene as Efficient Polymer Support for Palladium Nanoparticles. *J. Polym. Sci. Part A Polym. Chem.* **2015**, *53*, 5–9. [[CrossRef](#)]
27. Yang, K.; Niu, H.; Shi, Z.; Tan, R.; Li, T.; Shen, K.; Li, Y. Convenient Synthesis of Versatile Syndiotactic Polystyrene Materials Containing Pendant Alkenyl Groups with a Scandium Catalyst System. *Polym. Chem.* **2018**, *9*, 3709–3713. [[CrossRef](#)]
28. Guo, F.; Wang, B.; Ma, H.; Li, T.; Li, Y. Scandium-catalyzed Synthesis of Si–H-containing Syndiotactic Polystyrene and Its Functionalized Polymer Carrying Pendant Perylene Bisimide Units. *J. Polym. Sci. Part A Polym. Chem.* **2016**, *54*, 735–739. [[CrossRef](#)]
29. Wang, Z.; Liu, D.; Cui, D. Statistically Syndioselective Coordination (Co)polymerization of 4-Methylthiostyrene. *Macromolecules* **2016**, *49*, 781–787. [[CrossRef](#)]
30. Zhang, Z.; Dou, Y.; Li, S.; Cui, D. Highly Syndioselective Coordination (Co)polymerization of Isopropenylstyrene. *Polym. Chem.* **2018**, *9*, 4476–4482. [[CrossRef](#)]
31. Li, S.; Yan, F.; Zhang, Z.; Dou, Y.; Zhang, W.; Cui, D. Syndioselective Polymerization of Vinyl naphthalene. *Macromol. Rapid. Commun.* **2019**, *40*, 1900061. [[CrossRef](#)] [[PubMed](#)]
32. Schellenberg, J.; Tomotsu, N. Syndiotactic Polystyrene Catalysts and Polymerization. *Prog. Polym. Sci.* **2002**, *27*, 1925–1982. [[CrossRef](#)]
33. Schellenberg, J. Recent Transition Metal Catalysts for Syndiotactic Polystyrene. *Prog. Polym. Sci.* **2009**, *34*, 688–718. [[CrossRef](#)]
34. Rodrigues, A.S.; Kirillov, E.; Carpentier, J.F. Group 3 and 4 Single-site Catalysts for Stereospecific Polymerization of Styrene. *Coord. Chem. Rev.* **2008**, *252*, 2115–2136. [[CrossRef](#)]
35. Kim, Y.; Park, S.; Han, Y.; Do, Y. Syndiotactic Polymerization of Amino-functionalized Styrenes Using (Pentamethylcyclopentadienyl)titanatrane/MMAO Catalyst System. *Bull. Korean Chem. Soc.* **2004**, *25*, 1648–1652.
36. Grassi, A.; Longo, P.; Proto, A.; Zambelli, A. Reactivity of Some Substituted Styrenes in the Presence of a Syndiotactic Specific Polymerization Catalyst. *Macromolecules* **1989**, *22*, 104–108. [[CrossRef](#)]
37. Soga, K.; Nakatani, H.; Monoi, T. Copolymerization of Styrene and Substituted Styrenes with Tetramethoxytitanium-methylaluminoxane Catalyst. *Macromolecules* **1990**, *23*, 953–957. [[CrossRef](#)]
38. Napoli, M.; Grisi, F.; Longo, P. Half-Titanocene-Based Catalysts in the Syndiospecific Polymerization of Styrenes: Possible Oxidation States of the Titanium Species and Geometries of the Active Sites. *Macromolecules* **2009**, *42*, 2516–2522. [[CrossRef](#)]
39. Galdi, N.; Albuñia, A.R.; Oliva, L.; Guerra, G. Polymorphism of Syndiotactic Poly(*p*-fluoro-styrene). *Polymer* **2009**, *50*, 1901–1907. [[CrossRef](#)]
40. Longo, P.; Proto, A.; Zambelli, A. Syndiotactic Specific Polymerization of Styrene: Driving Energy of the Steric Control and Reaction Mechanism. *Macromol. Chem. Phys.* **1995**, *196*, 3015–3029. [[CrossRef](#)]
41. Zhou, Q.; Liang, H.; Wei, W.; Meng, C.; Long, Y.; Zhu, F. Synthesis of Amphiphilic Diblock Copolymers of Isotactic Polystyrene-block-isotactic Poly(*p*-hydroxystyrene) Using a Titanium Complex with an [OSSO]-type Bis(phenolate) Ligand and Sequential Monomer Addition. *RSC Adv.* **2017**, *7*, 19885–19893. [[CrossRef](#)]
42. Natta, G.; Pino, P.; Corradini, P.; Danusso, F.; Mantica, E.; Mazzanti, G.; Moraglio, G. Crystalline High Polymers of α -Olefins. *J. Am. Chem. Soc.* **1955**, *77*, 1708–1710. [[CrossRef](#)]
43. Maréchal, J.M.; Carlotti, S.; Shcheglova, L.; Deffieux, A. Stereospecific Anionic Polymerization of Styrene Initiated by R_2Mg /ROMt 'ate' Complexes. *Polymer* **2004**, *45*, 4641–4646. [[CrossRef](#)]

44. Liu, D.; Yao, C.; Wang, R.; Wang, M.; Wang, Z.; Wu, C.; Lin, F.; Li, S.; Wan, X.; Cui, D. Highly Isoselective Coordination Polymerization of *ortho*-Methoxystyrene with β -Diketiminato Rare-Earth-Metal Precursors. *Angew. Chem. Int. Ed.* **2015**, *54*, 5205–5209. [[CrossRef](#)] [[PubMed](#)]
45. Chai, Y.; Wang, L.; Liu, D.; Wang, Z.; Run, M.; Cui, D. Polar-Group Activated Isospecific Coordination Polymerization of *ortho*-Methoxystyrene: Effects of Central Metals and Ligands. *Chem. Eur. J.* **2019**, *25*, 2043–2050. [[CrossRef](#)]
46. Jiang, Y.; Zhang, Z.; Li, S.; Cui, D. Isospecific (Co)polymerization of Unmasked Polar Styrenes by Neutral Rare-Earth Metal Catalysts. *Angew. Chem. Int. Ed.* **2022**, *61*, e202112966. [[CrossRef](#)]
47. Rodrigues, A.S.; Kirillov, E.; Roisnel, T.; Razavi, A.; Vuillemin, B.; Carpentier, J.F. Highly Isospecific Styrene Polymerization Catalyzed by Single-Component Bridged Bis(indenyl) Allyl Yttrium and Neodymium Complexes. *Angew. Chem. Int. Ed.* **2007**, *46*, 7240–7243. [[CrossRef](#)]
48. Annunziata, L.; Rodrigues, A.S.; Kirillov, E.; Sarazin, Y.; Okuda, J.; Perrin, L.; Maron, L.; Carpentier, J.F. Isoselective Styrene Polymerization Catalyzed by ansa-Bis(indenyl) Allyl Rare Earth Complexes. Stereochemical and Mechanistic Aspects. *Macromolecules* **2011**, *44*, 3312–3322. [[CrossRef](#)]
49. Capacchione, C.; Proto, A.; Ebeling, H.; Mulhaupt, R.; Moller, K.; Spaniol, T.P.; Okuda, J. Ancillary Ligand Effect on Single-Site Styrene Polymerization: Isospecificity of Group 4 Metal Bis(phenolate) Catalysts. *J. Am. Chem. Soc.* **2003**, *125*, 4964–4965. [[CrossRef](#)]
50. Beckerle, K.; Manivannan, R.; Spaniol, T.P.; Okuda, J. Living Isospecific Styrene Polymerization by Chiral Benzyl Titanium Complexes That Contain a Tetradentate [OSSO]-Type Bis(phenolato) Ligand. *Organometallics* **2006**, *25*, 3019–3026. [[CrossRef](#)]
51. Nakata, N.; Toda, T.; Saito, Y.; Watanabe, T.; Ishii, A. Highly Active and Isospecific Styrene Polymerization Catalyzed by Zirconium Complexes Bearing Aryl-substituted [OSSO]-Type Bis(phenolate) Ligands. *Polymers* **2016**, *8*, 31. [[CrossRef](#)] [[PubMed](#)]
52. Paradiso, V.; Capaccio, V.; Lamparelli, D.H.; Capacchione, C. [OSSO]-bisphenolate Metal Complexes: A Powerful and Versatile Tool in Polymerization Catalysis. *Coord. Chem. Rev.* **2021**, *429*, 213644. [[CrossRef](#)]
53. McNeill, I.; Coskun, M. Structure and Stability of Halogenated Polymers: Part 4—Chain Brominated Polystyrene. *Polym. Degrad. Stab.* **1989**, *25*, 1–9. [[CrossRef](#)]
54. Kawaguchi, H.; Sumida, Y.; Muggee, J.; Vogl, O. Head-to-head Polymers: 19. Chlorination of *Cis*-1,4-polybutadiene. *Polymer* **1982**, *23*, 1805–1814. [[CrossRef](#)]
55. Wiacek, M.; Jurczyk, S.; Kurcok, M.; Janeczek, H.; SchabBalcerzak, E. Synthesis of Polystyrene Modified with Fluorine Atoms: Monomer Reactivity Ratios and Thermal Behavior. *Polym. Eng. Sci.* **2014**, *54*, 1170–1181. [[CrossRef](#)]
56. Sessions, L.; Cohen, B.; Grubbs, R. Alkyne-Functional Polymers through Sonogashira Coupling to Poly(4-bromostyrene). *Macromolecules* **2007**, *40*, 1926–1933. [[CrossRef](#)]
57. Jaymand, M. Recent Progress in the Chemical Modification of Syndiotactic Polystyrene. *Polym. Chem.* **2014**, *5*, 2663–2690. [[CrossRef](#)]
58. Shin, J.; Chang, Y.; Nguyen, T.; Noh, S.; Bae, C. Hydrophilic Functionalization of Syndiotactic Polystyrene via A Combination of Electrophilic Bromination and Suzuki–Miyaura Reaction. *J. Polym. Sci. Part A Polym. Chem.* **2010**, *48*, 4335–4343. [[CrossRef](#)]
59. Buonerba, A.; Fienga, M.; Milione, S.; Cuomo, C.; Grassi, A.; Proto, A.; Capacchione, C. Binary Copolymerization of *p*-Methylstyrene with Butadiene and Isoprene Catalyzed by Titanium Compounds Showing Different Stereoselectivity. *Macromolecules* **2013**, *46*, 8449–8457. [[CrossRef](#)]
60. Milione, S.; Cuomo, C.; Capacchione, C.; Zannoni, C.; Grassi, A.; Proto, A. Stereoselective Polymerization of Conjugated Dienes and Styrene–Butadiene Copolymerization Promoted by Octahedral Titanium Catalyst. *Macromolecules* **2007**, *40*, 5638–5643. [[CrossRef](#)]
61. Dall Asta, A.; Ragin, L. Nonlinear Behavior of Dynamic Systems with High Damping Rubber Devices. *Eng. Struct.* **2008**, *30*, 3610–3618. [[CrossRef](#)]
62. Wang, Y.; Yan, H.; Huang, Z. Static and Dynamic Mechanical Properties of Chlorobutyl Rubber Composites with Variable Sulfur/Accelerator Ratio. *Mater. Des.* **2011**, *284–286*, 1938–1941. [[CrossRef](#)]
63. Cohen, R.E.; Ramos, A.R. Homogeneous and Heterogeneous Blends of Polybutadiene, Polyisoprene, and Corresponding Diblock Copolymers. *Macromolecules* **1979**, *12*, 131–134. [[CrossRef](#)]
64. Halasa, A.F. Preparation and Characterization of Solution SIBR via Anionic Polymerization. *Rubber Chem. Technol.* **1997**, *70*, 295–308. [[CrossRef](#)]
65. Halasa, A.F.; Gross, B.B.; Hsu, W.L. Multiple Glass Transition Terpolymers of Isoprene, Butadiene, and Styrene. *Rubber Chem. Technol.* **2010**, *83*, 380–390. [[CrossRef](#)]
66. Zhu, S.H.; Chan, C.M.; Wong, S.C.; Mai, Y.W. Mechanical Properties of PVC/SBR Blends Compatibilized by Acrylonitrile-Butadiene Rubber and Covulcanization. *Polym. Eng. Sci.* **1999**, *39*, 1998–2006. [[CrossRef](#)]
67. Bochmann, M. The Chemistry of Catalyst Activation: The Case of Group 4 Polymerization Catalysts. *Organometallics* **2010**, *29*, 4711–4740. [[CrossRef](#)]
68. Bryliakov, K.P.; Talsi, E.P.; Voskoboinikov, A.Z.; Lancaster, S.J.; Bochmann, M. Formation and Structures of Hafnocene Complexes in MAO- and $\text{AlBu}^i_3/\text{CPh}_3[\text{B}(\text{C}_6\text{F}_5)_4]$ -Activated Systems. *Organometallics* **2008**, *27*, 6333–6342. [[CrossRef](#)]
69. Bochmann, M.; Lancaster, S.J. Monomer–Dimer Equilibria in Homo- and Heterodinuclear Cationic Alkylzirconium Complexes and Their Role in Polymerization Catalysis. *Angew. Chem. Int. Ed.* **1994**, *33*, 1634–1637. [[CrossRef](#)]